Analyzing the Role of Microgrids to Mitigate the Effects of Forecasting Error of Renewable Distributed Generators

Juan. M. Lujano-Rojas, José A. Domínguez-Navarro, and José M. Yusta
University of Zaragogoza, Zaragoza, Spain
lujano.juan@gmail.com; jadona@unizar.es; jmyusta@unizar.es

Gerardo J. Osório and Sérgio F. Santos
C-MAST/UBI, Covilha, Portugal
gjosilva@gmail.com; sdfsantos@gmail.com

Mohamed Lotfi and João P. S. Catalão
Faculty of Engineering of the University of Porto (FEUP) and INESC TEC, Porto 4200-465, Portugal
mohd.f.lotfi@gmail.com; catalao@fe.up.pt

***Abstract*— In this study, the operation of an energy system composed of a battery energy storage system (BESS) and a conventional generator to compensate the forecasting error of renewable power production has been analyzed. A scenario with low forecasting error and another with high forecasting error have been synthetically modeled and incorporated to a computational model of the energy system. The results obtained from a case study suggest that a low forecasting error could be compensated by a single BESS. However, a high forecasting error would require the installation of a controllable power source such as a conventional generator.**

Keywords—battery energy storage system, distributed generation, error forecasting, renewable energy.

I. NOMENCLATURE

d	Index for the day ($d = 1, \dots, D$=365).
h	Index for the hour of the day ($h = 1, \dots, H$=24).
l	Index for each scenario ($l = 1, \dots, L$).
t	Index for hour of the year ($t = 1, \dots, T$ = 8760).
$v_{(d,h)}$	Wind profile of day d and hour h (m/s).
$v_{(d)}^{max}$	Maximum wind speed of day d (m/s).
$\bar{v}_{(d,h)}$	Normalized profile of day d and hour h (m/s).
$x_{(d,h,l)}$, $z_{(d,h,l)}$	Random variables of day d, hour h, and scenario l.
a	Autocorrelation coefficient.
b	Random number.
$\mu_{(d)}$	Mean of the normalized wind profile of day d.
$\sigma_{(d)}$	Standard deviation of the normalized wind profile of day d.
$y_{(d,h)}$	Random variable of day d and hour h.
$\alpha_{(d)}$, $\beta_{(d)}$	Coefficients of beta distribution of day d.
$F_N(\cdot)$	Cumulative function of a normal distribution.
$F_\beta(\cdot)$	Cumulative function of a beta distribution.
$s_{(d,h,l)}$	Wind profile of day d, hour h, and scenario l (m/s).
$\bar{s}_{(d,h,l)}$	Normalized wind profile of day d, hour h, and scenario l (m/s).
$w_{(d,h)}$	Simulated wind speed of day d and hour h (m/s).
$u_{(t)}$	Wind speed at time t (m/s).
P_W^{max}	Rated power of wind turbine (kW).
v_I	Cut-in wind speed of wind turbine (m/s).
v_R	Rated wind speed of wind turbine (m/s).
v_O	Cut-off wind speed of wind turbine (m/s).
c, f, g	Parameters of wind turbine model.
Q	Control factor of charge controller.
$SOC_{(t)}$	SOC at time t.
SOC_B^{min}	Minimum SOC setting.
SOC_B^{max}	Maximum SOC setting.
$P_{B(t)}$	Battery power at time t (kW).
P_B^{max}	Cell stack rating power (kW).
E_B	Rated capacity of VRFB (kWh).
η_B	Efficiency of VRFB.
$P_{I(t)}$	Power of converter at time t (kW).
P_I^{max}	Rated power of converter (kW).
$\eta_{I(t)}$	Efficiency of power converter at time t.
$P_{G(t)}$	Gen set output power at time t (kW).
$P_{DL(t)}$	Dump load power at time t (kW).
i,j	Parameters of charge controller model.
m,n	Parameters of power converter model.
$P_{DL(t)}$	Dump load time series at time t (kW).
$P_{SG(t)}$	Power supplied to SG at time t (kW).
P_G^{min}	Minimum power of generator (kW).
P_G^{max}	Maximum power of generator (kW).
$u_{ACT(t)}$	Actual wind speed at time t (m/s).
$u_{FOR(t)}$	Forecasted wind speed at time t (m/s).
$P_{ACT(t)}$	Actual power at time t (kW).
$P_{FOR(t)}$	Forecasted power at time t (kW).

II. INTRODUCTION

Forecasting is crucial for optimal management of energy systems. Using information on environmental variables, energy consumption patterns, and the energy market, appropriate operation of the energy system can be achieved. Forecasting of wind and solar energies can be utilized in a centralized or decentralized manner depending on the energy system in question.

Centralized forecasting is typically used by power system operators for control of renewable generators within a balancing area, while decentralized forecasting corresponds to individual plant operators [1]. Forecasting techniques currently used, such as model output statistics (MOS), are based on physical and meteorological measurements incorporated in numerical weather prediction models, with regression analysis used for statistical post-processing of the output data [2].

The combined employment of these processes is suitable for use in optimal operation of power systems with renewable generation. However, renewable resources are not fully predictable which poses a critical limitation on the massive integration of wind and solar generation, both in centralized [3] and decentralized manners [4].

M. Lotfi and J.P.S. Catalão acknowledge the support by FEDER funds through COMPETE 2020 and by Portuguese funds through FCT, under 02/SAICT/2017 (POCI-01-0145-FEDER-029803).

978-1-7281-0653-3/19/$31.00 ©2019 IEEE

Since forecasting errors cannot be avoided, they are incorporated as a factor in the optimization problem which is formulated to determine optimal operation of energy systems. In the case of centralized systems, incorporation of wind and solar generation, as well as load demand, using various representative scenarios has been widely suggested in the literature [5]. Moreover, with the advent of the smart grid (SG) where residential consumers could act as distributed power generators, adoption of wind and solar energy at distribution level has been also highly supported. In this sense, approaches such as distributed generation (DG) and virtual power plant (VPP) [6] have gained attention due to their important enabling role in the incorporation of renewable resources.

In this regard, VPP control has been studied in the literature by many authors, especially its participation in electricity markets in order to gain an economic benefit. In [7], a two-stage stochastic programming method is employed to determine the optimal schedule of a VPP enrolled in spinning reserve and balancing markets. Measures such as conditional value-at-risk are used for investment risk-assessment. A three-stage stochastic bi-level optimization approach was proposed in [8] and [9], where management of demand response resources was also included.

In [10], representation of a VPP incorporating the forecasting error of several variables of interest related to electricity market operation and load demand were studied. The impact of forecasting error was accounted for by means of several representative scenarios included on a mixed-integer nonlinear programming approach. In [11], degradation of the battery energy storage system (BESS) associated with the VPP structure was modeled. This was done by means of a piecewise linear function, which is later incorporated on the optimal control analysis formulated as a two-stage stochastic mixed-integer linear programming problem. Moreover, in [12], VPP control was analyzed by combining confidence bounds and scenarios with a stochastic adaptive robust optimization model.

It is worthy to mention that much of the work found in literature was based on optimization techniques requiring a linearization process. This represents neither the operation of charge controller of BESS, nor its power converter. On the other hand, with massive integration of distributed renewable generation in the SG, the added variability could be challenging to manage by the system operator.

In such scenario, this study focuses on attempting to minimize the forecasting error of power produced by a microgrid composed of a conventional generator, a vanadium redox flow battery (VRFB), and a wind generator (WG). In addition, complex processes of the VRFB, charge controller, and power converter have all been incorporated.

The rest of this manuscript is organized as follows: Section III describes the procedure used for simulating the wind speed forecasting error. Section IV explains the mathematical model of the energy system. Section V describes the control strategy to minimize the wind power forecasting error, which is later illustrated on a case study presented in Section VI. Finally, conclusions are discussed in Section VII.

III. Forecasting Error Simulation

In order to incorporate forecasting errors, the prediction process first needs to be simulated.

A simple approach was used to simulate wind resource prediction (and error thereof) from a given time series using the following algorithm [13]:

- Step 1: Analyze the first day setting $d \leftarrow 1$.
- Step 2: For the day under study (d), estimate the maximum value of wind speed over the day as (1),

$$v_{(d)}^{max} = max\{v_{(d,h)} \; \forall \; h = 1, \dots, H\} \quad (1)$$

- Step 3: Normalize the daily profile ($h = 1, \dots, H$) to obtain values within the interval [0, 1] as presented in (2),

$$\bar{v}_{(d,h)} = v_{(d,h)} / v_{(d)}^{max} \quad (2)$$

- Step 4: Generate L random scenarios according to (3), considering the correlation coefficient (a). The factor b is a random number whose mean is equal to zero and standard deviation is equal to $\sqrt{1-a^2}$.

$$x_{(d,h,l)} = a x_{(d,h-1,l)} + b \; \forall \; l = 1, \dots, L \quad (3)$$

- Step 5: Calculate the normalized profile of the day being simulated using (4), where the mean value ($\mu_{(d)}$) of the daily profile ($\bar{v}_{(d,h)} \; \forall \; h = 1, \dots, H$) and the corresponding standard deviation ($\sigma_{(d)}$) are considered.

$$y_{(d,h)} = \left(\bar{v}_{(d,h)} - \mu_{(d)}\right) / \sigma_{(d)} \quad (4)$$

- Step 6: Considering the mean and standard deviation used in Step 5, estimate the parameters of the equivalent beta distribution presented in (5) and (6),

$$\alpha_{(d)} = \left(\left(\left[1 - \mu_{(d)}\right]\mu_{(d)}^2\right) / \sigma_{(d)}^2\right) - \mu_{(d)} \quad (5)$$

$$\beta_{(d)} = \left(\left(1 - \mu_{(d)}\right) / \mu_{(d)}\right) - \alpha_{(d)} \quad (6)$$

- Step 7: Calculate the normalized L scenarios incorporating the behavior of the daily profile using (7),

$$z_{(d,h,l)} = x_{(d,h,l)} + y_{(d,h)} \; \forall \; h = 1, \dots, H; l = 1, \dots, L \quad (7)$$

- Step 8: Apply probability transformation shown in (8) and (9) to obtain scenarios following a beta distribution (F_β) with the parameters previously estimated in Step 6.

$$F_N\left(z_{(d,h,l)}\right) = F_\beta\left(\bar{s}_{(d,h,l)}\right) \quad (8)$$

$$\bar{s}_{(d,h,l)} = F_\beta^{-1}\left(F_N\left(z_{(h,l)}\right)\right) \quad (9)$$

- Step 9: Scale the L scenarios, ($\bar{s}_{(d,h,l)} \; \forall \; h = 1, \dots, H; l = 1, \dots, L$), obtained in Step 8 (Eq. (9)) in order to obtain a feasible daily profile, ($s_{(d,h,l)} \; \forall \; h = 1, \dots, H; l = 1, \dots, L$). The scaling process is shown in (10),

$$s_{(d,h,l)} = \bar{s}_{(d,h,l)}\left[v_{(d)}^{max}\right] \quad (10)$$

- Step 10: Apply *k-means++* clustering algorithm over the L scenarios obtained in Step 9 (Eq. (10)) in order to choose the closest scenario to the original daily profile ($v_{(d,h)} \; \forall \; h = 1, \dots, H$). The daily series obtained at this step (called $w_{(d,h)} \; \forall \; h = 1, \dots, H$) as result of the application of the clustering process, follows in some degree (but not exactly) the actual wind speed of the day under analysis. For this reason, it could be interpreted as a typical forecasting error.
- Step 11: IF ($d < D$): THEN, assign $d \leftarrow d + 1$ and go to Step 2; ELSE go to Step 12.
- Step 12: Once D daily profiles are obtained, a time series ($u_{(t)}$ with $T = 8760$ elements) is built by re-shaping the ($w_{(d,h)} \; \forall \; d = 1, \dots, D; h = 1, \dots, H$) daily profiles.

IV. Simulation of Energy System

Fig. 1 shows the generalized structure of a microgrid assumed for this work, with the aim of the correcting the forecast error for power generation of the connected wind turbine (WT). In this structure, BESS is used to compensate for the forecasting error (when WT produces excess energy). More immense variations between actual and forecasted power are managed using the conventional generator, which represents a controllable power source .

If the VRFB is fully charged, a dump load is incorporated to dissipate excess energy present at the time, so that energy balance is properly maintained. In subsequent sub-sections, the mathematical model of each component of this hybrid energy system is described.

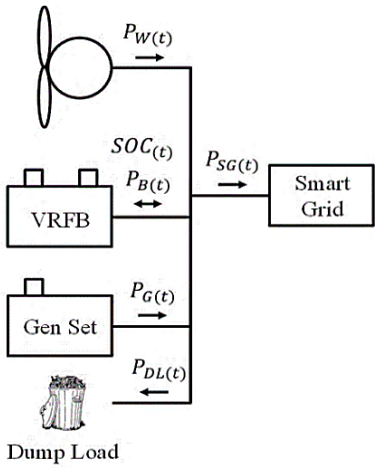

Fig. 1. Architecture of the hybrid energy system connected to SG.

A. Distributed Generation

The microgrid considered in this work is powered by wind generation. To model the WT, the generalized power curve proposed in [14] was used, as shown in (11)-(14),

$$P_{W(t)} = \begin{cases} 0, 0 \le u_{(t)} \le v_I, v_I > v_O \\ c + f(u_{(t)}) + g(u_{(t)})^2, v_I \le v_{(t)} \le v_R \\ P_W^{max}, v_R \le u_{(t)} \le v_O \end{cases} \quad (11)$$

$$c = \frac{1}{(v_I - v_R)^2}\left[v_I(v_I + v_R) - 4v_I v_R\left(\frac{v_I + v_R}{2v_R}\right)^3\right] \quad (12)$$

$$f = \frac{1}{(v_I - v_R)^2}\left[4(v_I + v_R)\left(\frac{v_I + v_R}{2v_R}\right)^3 - (3v_I + v_R)\right] \quad (13)$$

$$g = \frac{1}{(v_I - v_R)^2}\left[2 - 4\left(\frac{v_I + v_R}{2v_R}\right)^3\right] \quad (14)$$

B. Vanadium Redox Flow Battery

The BESS considered in this work is based on VRFB. The storage system architecture is described in Fig. 2, where the charge controller and power converter are shown. The amount of energy stored on the VRFB is measured by the state-of-charge (SOC), which is estimated using (15) [15],

$$SOC_{(t)} = SOC_{(t-1)} + (P_{B(t)}/E_B)\,\eta_B Q \quad (15)$$

The control factor Q models the influence of the charge controller on the amount of energy stored on the VRFB. SOC has to be limited between minimum (SOC_B^{min}) and maximum (SOC_B^{max}) values. These limits are maintained by the charge controller, which disconnects VRFB to prevent over-discharge and reduces charging power to maintain SOC below SOC_B^{max} (over-charge). These actions are modulated by factor Q, as represented in Eq. (16) [15].

$$Q = \begin{cases} max\left(1 - e^{\left[\left(\frac{i}{P_{B(t)}/P_B^{max}+j}\right)(SOC_{(t)} - SOC_B^{max})\right]}\right), P_{B(t)} > 0 \\ 1, P_{B(t)} < 0 \end{cases} \quad (16)$$

The charging efficiency (η_B) is variable as a function of power according to (17). This formulation provides the mathematical modeling of the power converter and represents how the BESS interacts with the rest of the system.

$$\eta_{I(t)} = \frac{P_{I(t)}}{mP_I^{max} + (1+n)P_{I(t)}} \quad (17)$$

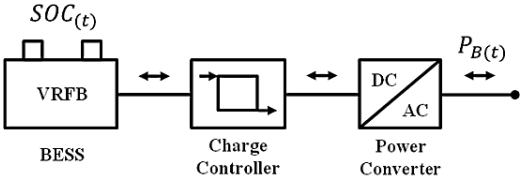

Fig. 2. Architecture of the BESS considered.

C. Conventional Generation

Low-capacity conventional generators were considered in this study, which are well established in technical literature. During operation, a typical conventional generator should produce power between minimum (P_G^{min}) and maximum (P_G^{max}) limits, recommended by manufacturers [16].

IV. Mitigating the Forecasting Error

The proposal of this work is to collectively employ the hybrid system components (shown in Fig. 1) with the aim of minimizing the forecasting error of WT output power. This is performed by implementing, the following algorithm:

- Step 1: Analyze the first hour of the year by setting $t \leftarrow 1$.
- Step 2: Read the actual ($u_{ACT(t)}$) and forecasted ($u_{FOR(t)}$) wind speed at time t. Evaluate these values on the power curve of Eqs. (11)-(14), obtaining the corresponding output power of WT, $P_{ACT(t)}$ (for the actual output power) and $P_{FOR(t)}$ (for the forecasted output power of WT).
- Step 3:
  IF ($P_{ACT(t)} > P_{FOR(t)}$), THEN charge VRFB with the excess energy defined as ($P_{ACT(t)} - P_{FOR(t)}$) and turn-off the conventional generator. With this strategy, actual wind generation is forced to be equal to the forecasted generation by storing the excess of energy on BESS.
  ELSEIF ($P_{ACT(t)} < P_{FOR(t)}$); THEN:
    IF ($P_{FOR(t)} - P_{ACT(t)} > P_G^{min}$), THEN turn-on conventional generator to compensate the forecasting error ($P_{FOR(t)} - P_{ACT(t)}$) and disconnect VRFB from microgrid.

ELSEIF ($P_{FOR(t)} - P_{ACT(t)} < P_G^{min}$), THEN turn-off the conventional generator and discharge VRFB to compensate the forecasting error.

- Step 4: If ($P_{FOR(t)} = P_{ACT(t)}$), the conventional generator is turn-off and VRFB is disconnected from microgrid.
- Step 5: IF (t < T); THEN assign $t \leftarrow t + 1$ and go to Step 2, ELSE stop.

V. Case Study

In this section, a hypothetical case study is used to analyze the proposed approach based on the architecture shown in Fig. 1. The system is composed of a WT of 100 kW (P_W^{max}=100 kW), with v_I=3 m/s, v_R=12 m/s, and v_O=25 m/s. Wind speed time series from 2005 in Eindhoven, The Netherlands, [17] was used to analyze the impact of wind resource forecasting system performance, shown in Fig. 3.

Using the procedure previously described in Section III, forecasting error of wind speed was simulated by considering two different cases: low error and high error. In both cases (low and high forecasting error) the autocorrelation coefficient was 0.9175, which corresponds to that of the time series in Fig. 3.

The VRFB has a cell stack power of 10 kW (P_B^{max}=10 kW), rated capacity of 5 kWh (E_B = 5 kWh), minimum SOC (SOC_B^{min}) of 0.15, maximum SOC (SOC_B^{max}) of 0.9, and conversion efficiency of 80% (η_B = 0.8). Rated power of conventional "*genset*" was assumed to be 10 kW (P_G^{max}), with a minimum limit of 2.5 kW (P_G^{min}).

A. Case 1: Low Forecasting Error

An example of a case with low forecasting error of wind speed is the results obtained by MOS forecasting. This was simulated by means of the process explained in Section III with $L = 10$, such that the *k-means++* clustering algorithm selects the random scenario which is closest time series of Fig. 3.

The obtained time series (actual and forecasted) were used as inputs for the WT model of Section IV-A in order to estimate wind generation. The results for both time series are shown in Fig. 4, while the histogram of the modeled forecasting error is presented in Fig. 5.

SOC and battery power time series are shown in Fig. 6 and 7, while power supplied by *genset* and power consumed by the dump load are presented in Fig. 8 and 9, respectively. As it can be observed, most of the power required to compensate the forecasting error is provided by BESS (Fig. 6 and 7). Meanwhile, the conventional generator is only switched off during higher deviations (Fig. 8).

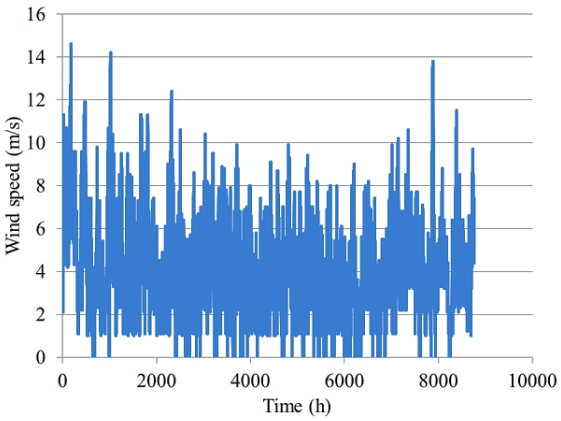

Fig. 3. Actual wind speed time series.

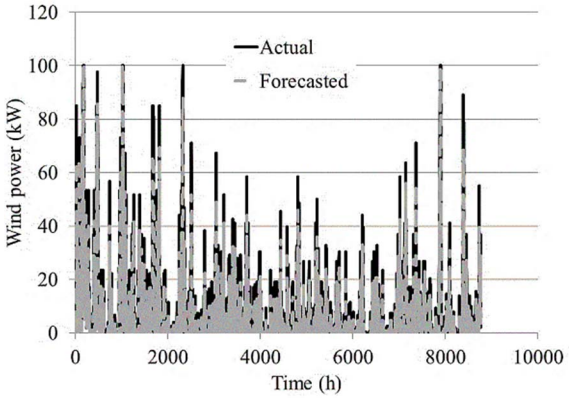

Fig. 4. Actual and forecasted wind power (low forecasting error).

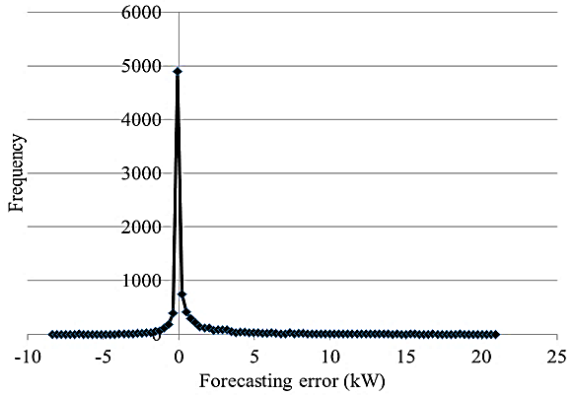

Fig. 5. Histogram of forecasting error (low forecasting error).

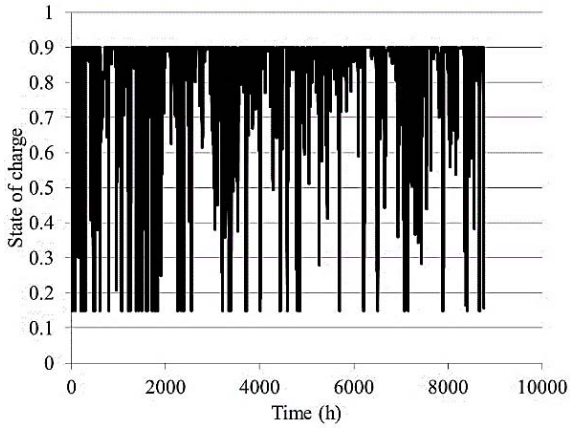

Fig. 6. SOC time series (low forecasting error).

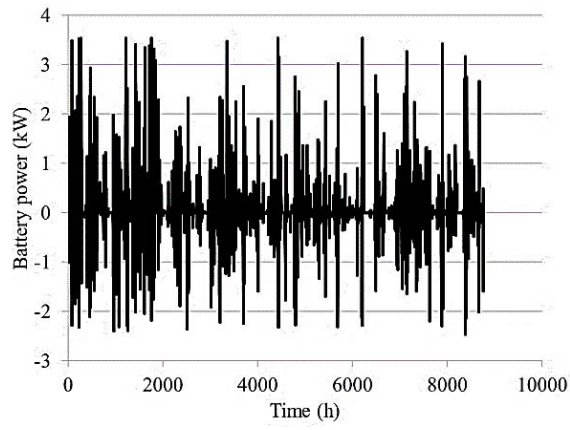

Fig. 7. Battery power time series (low forecasting error).

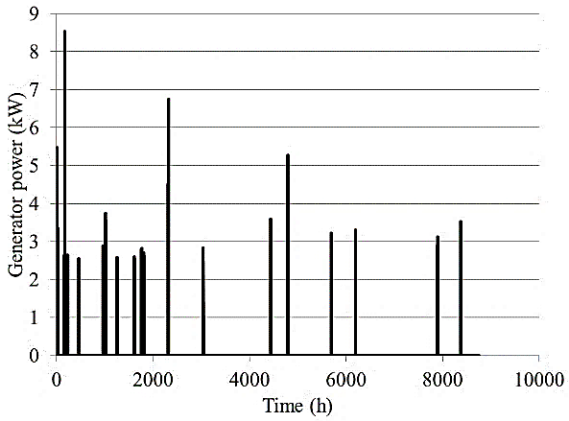

Fig. 8. Generator output power (low forecasting error).

B. Case 2: High Forecasting Error

As with the previous case, the simulation of a higher forecasting error was obtained by considering $L = 1$, such that the *k-means++* clustering algorithm directly selects only one random scenario provided. In other words, the resulting time series has an arbitrarily high forecasting error. Fig. 10 shows the wind power time series for this case and the corresponding is shown in Fig. 11. Fig. 12 shows the power time series.

The power provided by the conventional generator is presented in Fig. 13. The excess power dissipated by the dump load is presented in Fig. 14. Table I summarizes the results obtained for both analyses under low and high forecasting errors. In a general sense, the forecasting error has an important impact on the operation of the system. For low forecasting errors, the BESS is sufficient.

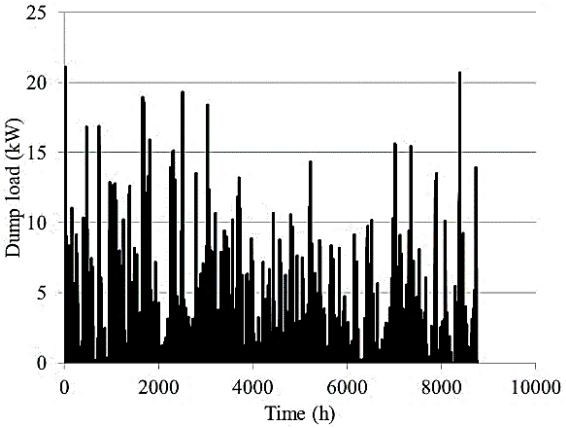

Fig. 9. Dump load power (low forecasting error).

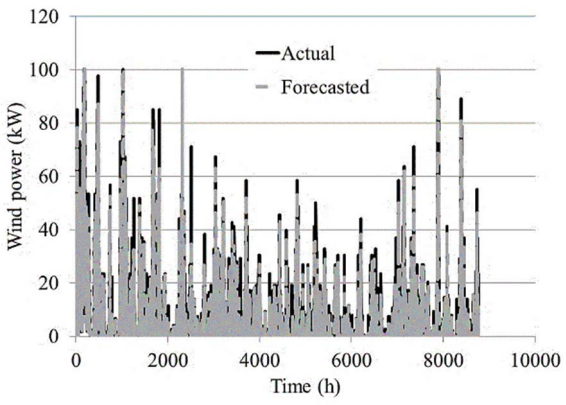

Fig. 10. Actual and forecasted wind power (high forecasting error).

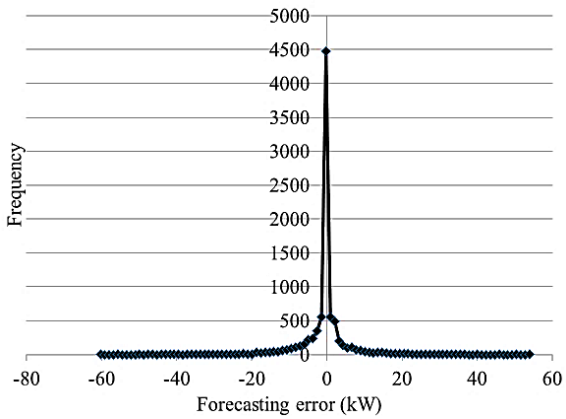

Fig. 11. Histogram of forecasting error (high forecasting error).

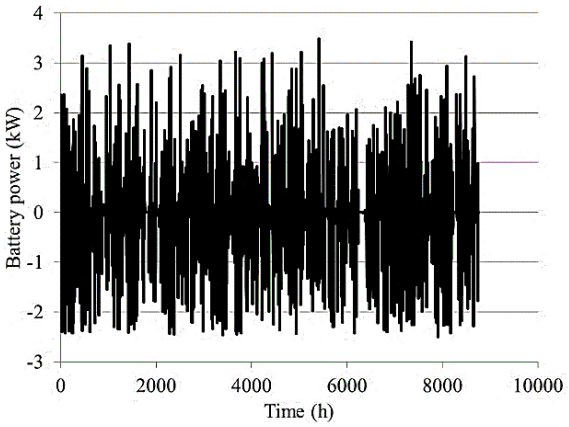

Fig. 12. Battery power time series (high forecasting error).

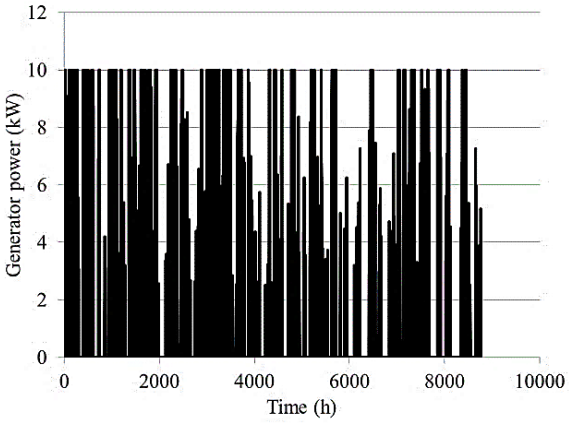

Fig. 13. Generator output power (high forecasting error).

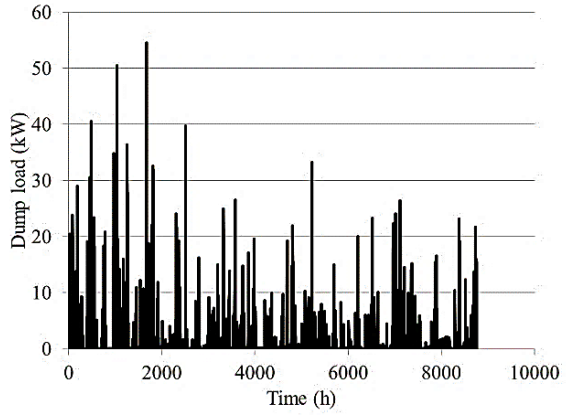

Fig. 14. Dump load power (high forecasting error).

TABLE I. ENERGY SYSTEM PERFORMANCE

Variable		Low Error	High Error
Forecasting error	(kW)	0.8048	2.8285
Charging power	(kWh/yr)	501.5521	987.3858
Discharging power	(kWh/yr)	662.6868	1461.5000
Generator power	(kWh/yr)	193.3307	10077.4780
Dump load power	(MWh/yr)	5.5730	9.7561

VI. CONCLUSIONS

In this work, the impact of renewable power forecasting error on the operation of a hybrid energy system has been studied. Wind speed forecasting error has been synthetically simulated by means of a first-order Markov model. Two different situations were considered: low and high forecasting error. According to the obtained results, a low forecasting error could be compensated with an adequately dimensioned BESS. However, systems with higher forecasting errors would require the incorporation of a conventional generation unit. The utilization of this architecture with DG units can effectively mitigate the negative influence of uncertainty introduced by renewable sources.

REFERENCES

[1] T. Tian, I. Chernyakhovskiy, "Forecasting wind and solar generation: improving system operations," *National Renewable Energy Laboratory*, NREL/FS-6A20-65728, Jan. 2016.

[2] L. Zjavka, "Numerical weather prediction revisions using the locally trained differential polynomial network," *Expert Syst. Appl.*, vol. 44, pp. 265-274, Feb. 2016.

[3] C. L. Archer, H. P. Simão, W. Kempton, W. B. Powell, M. J. Dvorak, "The challenge of integrating offshore wind power in the U.S. electric grid. Part I: Wind forecast error," *Renew. Energy*, vol. 103, pp. 346-360, Apr. 2017.

[4] H. Yi, M. H. Hajiesmaili, Y. Zhang, M. Chen, X. Lin, "Impact of the uncertainty of distributed renewable generation on deregulated electricity supply chain," *IEEE Trans. Smart Grid*, vol. 9, no. 6, pp. 6183-6193, Nov. 2018.

[5] Z. Q. Xie, T. Y. Ji, M. S. Li, Q. H. Wu, "Quasi-Monte Carlo based probabilistic optimal power flow considering the correlation of wind speeds using copula function," *IEEE Trans. Power Syst.*, vol. 33, no. 2, pp. 2239-2247, Mar. 2018.

[6] N. Etherden, V. Vyatkin, M. H. J. Bollen, "Virtual power plant for grid services using IEC 61850," *IEEE Trans. Ind. Infor.*, vol. 12, no. 1, pp. 437-447, Feb. 2016.

[7] S. R. Dabbagh, M. K. Sheikh-El-Eslami, "Risk assessment of virtual power plants offering in energy and reserve markets," *IEEE Trans. Power Syst.* vol. 31, no. 5, pp. 3572-3582, Sept. 2016.

[8] E. G. Kardakos, C. K. Simoglou, A. G. Bakistzis, "Optimal offering strategy of a virtual power plant: a stochastic bi-level approach," *IEEE Trans. Smart Grid*, vol. 7, no. 2, pp. 794-806, Mar. 2016.

[9] Q. Zhao, Y. Shen, M. Li, "Control and bidding strategy for virtual power plants with renewable generation and inelastic demand in electricity markets," *IEEE Trans. Sust. Energy*, vol. 7, no. 2, pp. 562-575, Apr. 2016.

[10] P. Karimyan, M. Abedi, S. H. Hosseinian, R. Khatami, "Stochastic approach to represent distributed energy resources in the form of a virtual power plant in energy and reserve markets," *IET Gen. Trans. Distr.*, vol. 10, no. 8, pp. 1792-1804, May 2016.

[11] B. Zhou, X. Liu, Y. Cao, C. Li, C. Y. Chung, K. W. Chan, "Optimal scheduling of virtual power plant with battery degradation cost," *IET Gen. Trans. Distr.,* vol. 10, no. 3, pp. 712-725, Mar. 2016.

[12] A. Baringo, L. Baringo, "A stochastic adaptive robust optimization approach for the offering strategy of a virtual power plant," *IEEE Trans. Power Syst.*, vol. 32, no. 5, pp. 3492-3504, Sept. 2017.

[13] HOMER Energy Support. Accessed on 16/10/2018. [Online]. Available: http://usersupport.homerenergy.com/

[14] P. Giorsetto, K. F. Utsurogi, "Development of a new procedure for reliability modeling of wind turbine generators," *IEEE Trans. Power Appar. Syst.*, vol. PAS-102, no. 1, pp. 134-143, Jan. 1983.

[15] G. J. Osório, E. M. G. Rodrigues, J. M. Lujano-Rojas, J. C. O. Matias, J. P. S. Catalão, "New control strategy for the weekly scheduling of insular power systems with a battery energy storage system," *Appl. Energy*, vol. 154, pp. 459-470, Sept. 2015.

[16] R. Dufo-López, J. L. Bernal-Agustín, "Influence of mathematical models in design of PV-diesel systems," *Energy Conv. Manag.*, vol. 49, no. 4 pp. 820-831, Apr. 2008.

[17] Royal Netherlands Meteorological Institute, *KNMI Hydra Project*. Accessed on 12/03/2018. [Online]. Available: http://www.knmi.nl